Toward Supervisory-Level Control for the Energy Consumption and Performance Optimization of Displacement-Controlled Hydraulic Hybrid Machines

Enrique Busquets and Professor Dr.-Ing. Monika Ivantysynova

Maha fluid power research center, Purdue University. 1500 Kepner Dr. Lafayette, IN. 47905. USA.
Email: ebusquet@purdue.edu, mivantys@purdue.edu

Abstract

Environmental awareness, production costs and operating expenses have provided a large incentive for the investigation of novel and more efficient fluid power technologies for decades. In the earth-moving sector, hydraulic hybrids have emerged as a highly efficient and affordable choice for the next generation hydraulic systems. Displacement-controlled (DC) actuation has demonstrated that, when coupled with hydraulic hybrids, the engine power can be downsized by up to 50% leading to substantial savings. This concept has been realized by the authors' group on an excavator prototype where a secondary-controlled hydraulic hybrid drive was implemented on the swing. Actuator-level controls have been formulated by the authors' group but the challenge remains to effectively manage the system on the supervisory-level. In this paper, a power management controller is proposed to minimize fuel consumption while taking into account performance. The algorithm, a feedforward and cost-function combination considers operator commands, the DC actuators' power consumption and the power available from the engine and hydraulic hybrid as metrics. The developed strategy brings the technology closer to the predicted savings while achieving superior operability.

KEYWORDS: Hydraulic Hybrids, Power Management, Displacement-control

1. Introduction

Off-highway vehicles' systems have been the subject of extensive engineering research over the past few decades. Novel architectures and control algorithms have been developed to maximize overall system performance and efficiency. The earthmoving equipment sector has demonstrated large improvements in both aspects and much attention has been paid to excavators due to their predominantly cyclical operation and large inertial forces. One approach to exploit these machines' operation are hybrid systems. Electric hybrid excavators were first introduced in the market by Kobelco and

Komatsu. In their systems, an electric motor is installed as the swing drive actuator and an electric capacitor is installed for kinetic energy storage. These manufacturers have advertised up to 41% energy savings for specific working cycles /1/, /2/ and /3/. A large disadvantage electric hybrids is their high production cost. As an alternative, CAT has commercialized a hydraulic hybrid excavator /4/ in which swing braking energy is captured in a high pressure accumulator. Besides the commercially available hydraulic hybrid concepts, the authors' group at Purdue has studied, implemented and tested the concept of a secondary controlled hybrid swing drive /5/.

The concept of secondary control actuation was originally patented in /6/ as a more efficient alternative to valve controlled actuation. The concept employs a hydraulic unit to control the pressure at the working port of the units controlling the inertia loads, also known as secondary units, through a pressure-compensated mechanism. The secondary units' displacement control mechanisms are employed to control the inertia load dynamics. Depending on the operation, secondary units may operate as pumps or motors. To prevent these units from over speeding they must be controlled in a closed-loop fashion. In many instances a hydraulic accumulator is installed in the working line to add damping. However, the purpose of this component as originally proposed, is not to store energy. The hydraulic hybrid secondary-controlled drive proposed by the author's group /5/ follows the abovementioned underlying working principles of secondary-control. Nonetheless, the hydraulic architecture has been modified to include a hydraulic accumulator for energy storage and the pressure compensation system has been replaced with a direct-operated electro-hydraulic system. In this form, both hydraulic units are allowed to operate as pumps or motors. Ultimately this allows for the recuperation, storage and/or transmission of the secondary unit braking energy to the common engine shaft.

A constant pressure net is unreasonable for a secondary-controlled hydraulic hybrid drive /5/ /7/. With this in mind, the authors' group has developed a minimum speed and a rule-based control strategy for the power management of a hydraulic hybrid excavator. Nonetheless, these strategies were not able to achieve the predicted engine downsizing in implementation /8/. In this paper, an effective and general power management supervisory-level controller is developed for displacement-controlled hydraulic hybrid machines. The control strategy proves that, through the proper management of the primary unit, the system is able to perform as a conventional machine while operating with a downsized engine. Simulation results with a downsized engine and measurement results in an excavator prototype with a stock-sized engine show that the control strategy maintains the engine at or below the prescribed engine power for a truck-loading cycle.

2. Excavator Prototype System and Simulation Model

The machine under consideration is a Bobcat 435, 5-ton compact excavator. To accurately describe the machine dynamic behaviour a high-fidelity model is created in MATLAB SimMechanics. This model is combined with a hydraulic model where Simulink is used to calculate the forces and torques generated by the hydraulic system and SimMechanics feeds back the resulting dynamics. Additionally, a nonlinear model of the engine is created in the same interface. Overall, the models allow for the determination of the loads imposed on the engine through the hydraulic units and their effect on its rotational speed.

2.1. Hydraulic System

The working hydraulics of the studied excavator are shown in **Figure 1**.
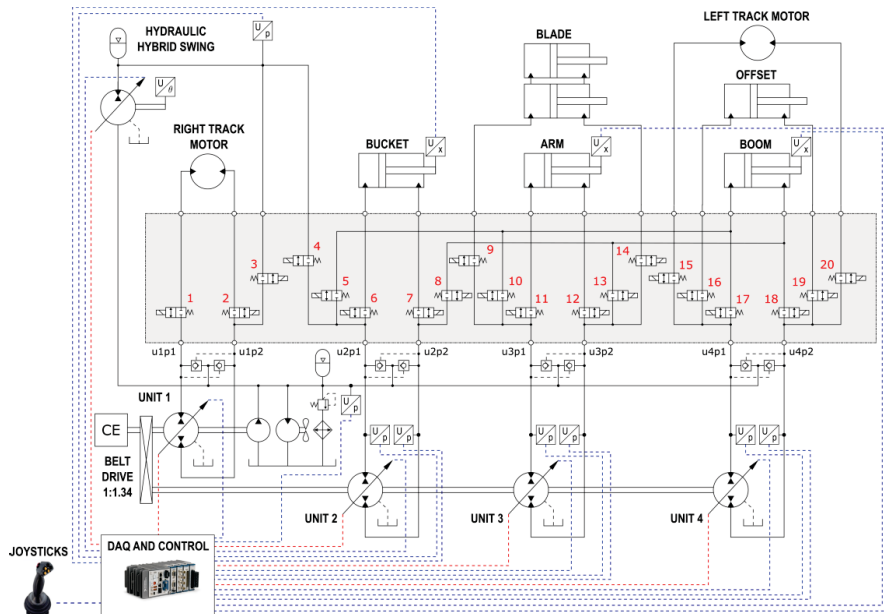

Figure 1: Hydraulic hybrid excavator prototype hydraulic circuit and instrumentation

They consist of four-18 cc/rev variable displacement axial piston machines, six single-rod linear actuators for the boom, arm, bucket, offset, and blade functions, two fixed displacement radial piston motors for the tracks and a variable displacement axial piston pump/motor for the secondary-controlled hybrid swing drive. For the simulation study, only the digging operation has been taken into account; therefore, valves 2, 3, 6, 7, 11, 12, 17 and 18 are opened according to the actuators' commanded motion while the rest remain closed. It follows that only the swing, boom, arm and bucket actuators are

modeled. These actuators' load dynamics can be expressed according to **Figure 2** as

$$\dot{p}_1 = \frac{K}{V_1}\left(Q_1 - Q_s + Q_{chk1} - A_1\dot{x} - Q_{Li} - Q_{r1}\right)$$

$$\dot{p}_2 = \frac{K}{V_2}\left(-Q_2 + Q_s - Q_{chk2} + A_2\dot{x} + Q_{Li} - Q_{r2}\right)$$

(1.1)

where p_1 and p_2 are the actuator bore and rod side pressures, V_1 and V_2 are the contained fluid volumes given by $V_1 = V_{dead} + A_{bore}x + V_L$ and $V_2 = V_{dead} - A_{rod}(x_{max} - x) + V_L$, where V_{dead} is the actuator dead volume, A_{bore} and A_{rod} are the bore and rod side areas respectively, x is the actuator position and its time derivative denotes its velocity, x_{max} is the actuator stroke, and V_L is the line volume. Also, K is the oil effective bulk modulus, Q_{Li} is the actuator internal leakage flow and Q_{r1} and Q_{r2} are the relief valves' flows, which are calculated using a linear flow coefficient based on catalogue data. The pump flows, Q_1 and Q_2, as well as their volumetric losses, Q_s, are obtained based on empirical loss models. The hydraulic units' dynamics have been modeled based on their control valves dynamics, which are of second order /9/. Finally, Q_{ck1} and Q_{ck2} are the pilot-operated (PO) check valves' flows, which may be expressed using the orifice equation and balancing the forces on the valve spool to find its position.
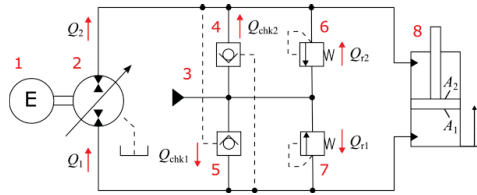

Figure 2: Displacement-controlled linear actuator hydraulic circuit

The hydraulic hybrid accumulator state of charge can be modeled as

$$\dot{p}_{hp} = \frac{1}{C_H}\left(n_1 V_1 \beta_1 - Q_{s1} - \dot{\varphi} i_{TOT} V_2 \beta_2 - Q_{s2}\right)$$

(1.2)

where n_1 is the primary unit speed, V_1, V_2, β_1 and β_2 are the primary and secondary units' maximum volumetric displacements and normalized displacements respectively, φ is the excavator cabin angular position and its time derivative denotes its angular velocity and i_{TOT} is the gear ratio between the secondary unit pinion and cabin ring gear. Finally, Q_{s1} and Q_{s2} are the primary and secondary unit's volumetric losses obtained based on empirical data and C_H is the hydraulic capacitance expressed in terms of V_o, the accumulator gas volume, N, the assumed ideal gas polytropic exponent, and p_o, the accumulator pre-charge, as $C_H = (V_o/N)\cdot(p_o^N/p_{hp}^{(N+1)/N})$.

2.2. Mechanical System

The excavator prototype mechanical system has been modelled in SimMechanics according to CAD data and the components' inertia tensors. The, the swing dynamics on the other hand have been modelled as

$$J\left(x_{arm}, x_{boom}, x_{bucket}\right)\ddot{\varphi} = V_M dp i_{TOT} \beta_M - b\dot{\varphi} - T_c \text{sign}\left(\dot{\varphi}\right) \tag{1.3}$$

where $J(x_{arm}, x_{boom}, x_{bucket})$ is the inertia of the excavator cabin, which is a function of the arm, boom and bucket actuator positions x_{arm}, x_{boom}, and x_{bucket}, φ is the excavator cabin angular position with its first and second time derivatives denoting its velocity and acceleration, V_M is the hydraulic motor maximum volumetric displacement, dp is the motor differential pressure, i_{TOT} is the ratio between the hydraulic motor pinion and the cabin ring gear, β_M is the hydraulic motor normalized displacement, b is the viscous friction coefficient and T_c is the Coulomb friction coefficient.

2.3. Engine Model

The engine under study is a naturally aspirated 36.5 kW Kubota stock diesel engine with a maximum rated speed of 2700 rpm. It's dynamics, are given by

$$\dot{n}_e = \frac{1}{J_e}\left(M_{e\,eff} - M_L\right) \tag{1.4}$$

where n_e is the engine speed, J_e is the engine inertia, $M_{e\,eff}$ is the effective engine torque which can be expressed as $M_{e\,eff} = M_{e\,th} - M_f$, where $M_{e\,th}$ is the engine theoretical torque output and M_f is the engine torque loss due to friction. Finally, M_L is the engine load torque. The maximum theoretical engine torque, $M_{e\,th}$, can be obtained from measured data of the engine wide-open-throttle (WOT), which includes friction. So, to get the maximum theoretical engine torque, the WOT measurements must be modified to remove the measured friction as $M_{e\,th} = u_E(M_{WOT} + M_f)$ where u_E is the normalized engine control input at any operating engine speed and M_{WOT} is the measured WOT curve torque. The engine friction on the other hand is modeled based on published empirical data /10/ of the effective mean pressure as $p_{me} = 75 + 0.048n_e + 0.4S_p^2$ and knowing that the effective mean pressure is given by $p_{me} = 2\pi M n_e/V_{eng}$ where V_{eng} is the engine displacement in liters and M is the resulting torque from the mean effective pressure, the torque loss due to friction can be expressed as

$$M_f = \frac{V_{eng}}{2 \cdot 2\pi}\left(75 + 0.048n_e + 0.4S_p^2\right) \tag{1.5}$$

where S_p is the pistons' speed in m/s. This parameter can be expressed for a four-stroke engine and taking into account the engine piston stroke, l, as $S_p = n_E 2l/60$.

3. Supervisory-Level Control Development

The proposed supervisory controller comprises two parts, 1) an instantaneous optimization for the minimization of fuel consumption and maximization of actuator performance and 2) a feedforward controller for the hydraulic hybrid primary unit based on the system power flows. In conjunction, these two parts optimize the usage of engine power and allow the hybrid to provide complementary power to the common shaft.

3.1. The Engine Power Management Control Strategy

The engine power management control is similar to that in /11/ wherein the efficiency characteristics of the engine as well as the hydraulic units are taken into account to minimize fuel consumption and satisfy machine transient performance. With this algorithm the engine speed will change to suit efficiency and performance parameters, which differs from traditional mobile equipment operation where the operator sets a fixed reference engine speed. In doing so, the algorithm takes advantage of the fact that diesel engines are more efficient at large torque loads but low speeds and hydraulic units are more efficient at low speeds and large displacements. The controller formulation revolves around the minimization of and objective function at each moment in time. For DC hydraulic hybrid systems the proposed formulation can be expressed as

$$J = \text{bsfc}\left(n_e, M_e\right) + k_Q \sum_{i=1}^{n} Q_{\text{DC err}, i} \tag{1.6}$$

where $\text{bsfc}(n_e, M_e)$ is the engine brake specific fuel consumption, k_Q is a flow rate error gain for performance adjustment, and the flow rate error can be formulated based on the desired and current DC flows, $Q_{\text{DC, des}}$, and $Q_{\text{DC, curr}}$ respectively, as

$$Q_{\text{DC err}} = \begin{cases} 0 & \left|Q_{\text{DC, des}}\right| \leq Q_{\text{p, curr}} \\ \left|Q_{\text{DC, des}}\right| - Q_{\text{p, current}} & \left|Q_{\text{DC, des}}\right| > Q_{\text{p, curr}} \end{cases} \tag{1.7}$$

Equation (1.6) yields a nonlinear, multivariable optimization subject to flow rate constraints $(\beta_{\text{ref}}, n_{e, \text{ref}}) = f(dp, Q_{\text{DC, curr}})$, speed constraints $n_{e, \min} \leq n_e \leq n_{e, \max}$ and torque constraints $T_e \leq T_{e, \max}(n_e)$. To simplify the task of solving this optimization scheme, the flow rate constraint can be directly substituted into Eq. (1.6), the torque constraint can be implicitly enforced by adding a penalty, J_c, to Eq. (1.6) and the speed constraint is a bound on the optimized parameter. An option for the implementation of the proposed approach is to pre-calculate the optimal speed trajectories into a lookup table.

Nonetheless, due to the large number of states in the system, an online solution is preferred. The optimization problem is solved online at a sampling rate of 25 Hz using a golden section (Fibonacci) search. It is evident that a trade-off between efficiency and performance will exist due to the much slower dynamics of the engine relative to the DC actuators. Nevertheless, different values for the parameter k_Q may be prescribed to establish different machine operating modes such as energy saving (k_Q is small) or performance (k_Q is large).

An additional requirement on the engine power management is an anti-stall function. The author's group has developed an anti-stall control for DC systems which scales the units' displacements based on the engine speed error and their contributing torque load. More details on this controller can be found in /12/.

3.2. The Hydraulic Hybrid Power Management Control

The formulation of the hydraulic hybrid supervisory controller is achieved by noting the energy flows in the system. In reference to **Figure 3**, it can be observed that the chosen convention takes into account power going into the common engine shaft as positive and power consumed as negative. It is then observed that energy stored in the hybrid accumulator, E_A, must be transferred to the engine shaft through the primary unit as P_P, when the engine power, P_e, is less than that demanded by the DC actuators, P_{DC}. It is important to note that the secondary unit power, P_S, depends mainly on the operator commands. Each of the depicted energies can be expressed as shown in Eq. (1.8) to Eq. (1.12).
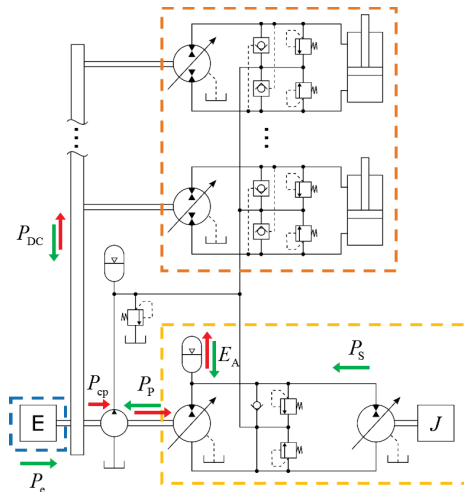
$$P_{DC} = \sum_{i=1}^{n} \Delta p_i n_e V_i \eta_i \beta_i \qquad (1.8)$$

$$P_S = p_{HP} n_S V_S \eta_S \beta_S \qquad (1.9)$$

$$P_e = M_e n_e \qquad (1.10)$$

$$E_A = \int_{V_2}^{V_0} p_{HP} dV \qquad (1.11)$$

$$P_{cp} = M_{cp} n_e \qquad (1.12)$$

Figure 3: Hydraulic hybrid DC energy flows

It can be further noted that $P_P = E_A/dt + P_S$ and $P_{DC} = P_e + P_P + P_{cp}$. It follows that the power required from the engine can be expressed as $P_e = P_{DC} - E_A/dt - P_S - P_{cp}$. Substituting the expressions in Eq. (1.8) to Eq. (1.12) and noting the expression in Eq. (1.2) allow us to see that the quantities used to control the system energy flows are the engine speed and the primary unit displacement, which is no surprise. On the other hand the DC actuator displacements and the secondary unit speed are performance parameters. It is then concluded that the control task for the supervisory controller is to stay close to the desired DC and hybrid energy levels while minimizing fuel consumption. To achieve this it is proposed to formulate a displacement command for the hybrid primary unit that is directly related to the power relations derived above. Such relations are given by

$$\beta_P = \left(\frac{P_{e\,max\,@\,min(bsfc)} - P_{DC}}{P_{e\,downsized\,max}} \right) \left(1 - S_A(p_A) \right) \quad \text{for } P_{e\,max\,@\,min(bsfc)} - P_{DC} \geq 0 \tag{1.13}$$

$$\beta_P = \left(\frac{P_{e\,max\,@\,min(bsfc)} - P_{DC}}{P_{DC\,max} - P_{e\,downsized\,max}} \right) \left(S_A(p_A) \right) \quad \text{for } P_{e\,max\,@\,min(bsfc)} - P_{DC} < 0 \tag{1.14}$$

In reference to Eq. (1.13), it can be observed that the expression takes the normalized amount of the current engine power, $P_{e\,max\,@\,min(bsfc)}$, which is not utilized by the DC actuators, P_{DC}, and commands the primary unit to charge the accumulator. This levels the engine at the highest allowable power when the accumulator must be charged. The relationship in Eq. (1.14) on the other hand takes the normalized difference between current engine power, $P_{e\,max\,@\,min(bsfc)}$, and the power demanded by the DC actuators, P_{DC}, and normalizes such value with respect to the maximum power above the downsized engine rated power. This in turn commands the primary unit to discharge the accumulator thereby complementing the engine power. It is important to note the scaling factor S_A is utilized to implicitly impose constraints on the amount of energy stored or taken from the hybrid accumulator by considering the accumulator pressure, p_A. During the discharging scenario this scaling factor allows the swing drive to retain operability and on the charging scenario it de-strokes the primary unit once a specified maximum charge limit has been reached. This last point is crucial for the accumulator integrity but also from the energy perspective to prevent wasting energy over a relief valve when the machine is not in use. It is also important to recognize that, due to the nature of the proposed approach and the hybrid architecture, the secondary unit power is automatically taken from the hydraulic accumulator or recaptured. This flexibility allows the controller to focus the control effort on providing enough power for the DC actuators while relying on the hybrid actuator-level controls and the abovementioned implicitly enforced constraints to meet a certain performance criteria.

4. Simulation Results for a Truck-Loading Cycle with Downsized Engine

To simulate the system behaviour, the derived control algorithms in section 3 were incorporated in the mathematical model described in section 2. The presented simulated results in **Figure 4** to **Figure 8** are the outcome of providing the simulation model with measured commanded actuator motions of an expert 90° truck-loading cycle. It can be observed that the main controller task has been achieved by completing the short digging cycle with 55% percent of the installed stock engine power. A detailed plot of the power throughout the system is shown in Figure 4. It can be observed that the power consumed by the DC circuit is above the maximum possible power provided by the downsized engine. To accomplish this, energy stored in the hybrid accumulator, also shown in Figure 4, is channelled to the common shaft by means of the primary unit working in motoring mode, as can be seen from its displacement in **Figure 5**. For near optimal engine power consumption, the engine speed, shown in Figure 8, varies over time according to the operator commands, thereby forcing the hydraulic units to operate at higher efficiencies. The engine characteristics and operation can be seen in **Figure 6**.
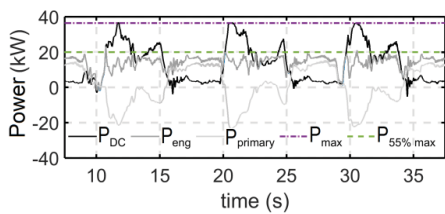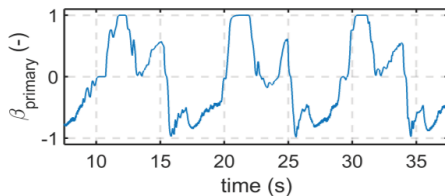

Figure 4: System power

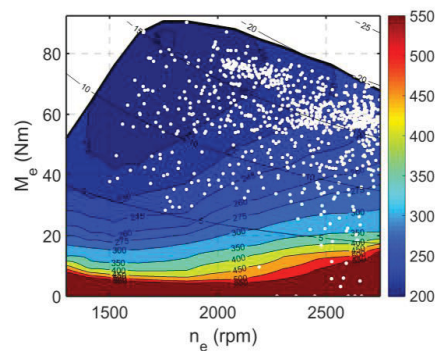**Figure 5**: Primary unit displacement
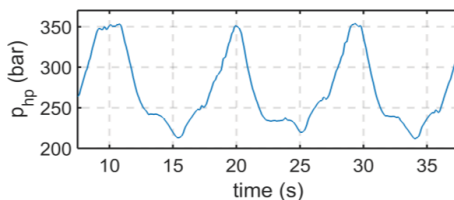
Figure 6: Engine Operation
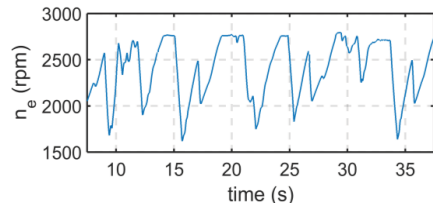

Figure 7: Accumulator pressure

Figure 8: Engine speed

In this particular case the performance demand results in high speed operation for a considerable part of the cycle; nonetheless, when possible, the engine speed is lowered.

5. Control Validation through Measurements on the Prototype Excavator

The aforementioned control algorithms were implemented in the excavator prototype described in section 2. The hardware and data acquisition was conducted using National Instruments devices at 300 Hz and the instantaneous optimization algorithm in section 3.1 was executed at 25 Hz. In reference to the results presented in **Figure 9** through **Figure 13**, the combination of power management controllers effectively allows a short digging cycle to be completed with 55% of the stock engine power. In Figure 9, it can be observed that the engine power never increases above the prescribed downsized maximum power of 20 kW. The DC actuators power demand on the other hand does increase above this threshold. This operation is possible through the addition of the complimentary hydraulic hybrid power into the common shaft, also shown in Figure 9.
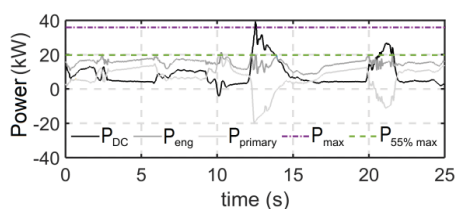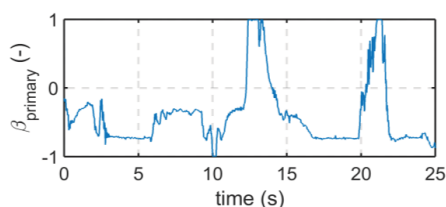

Figure 9: System power

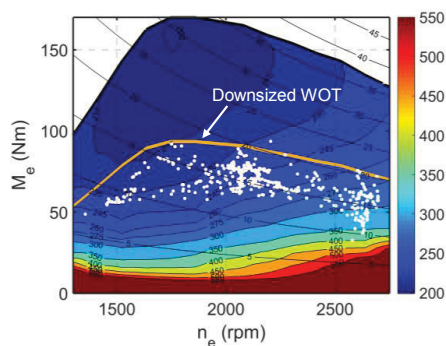**Figure 10**: Primary unit displacement
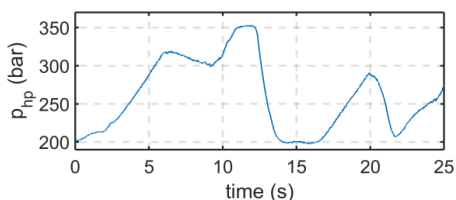
Figure 11: Engine Operation
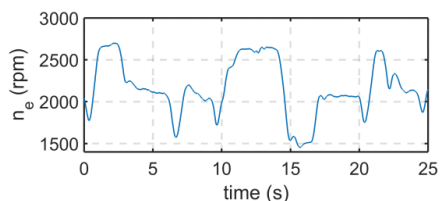

Figure 12: Accumulator pressure

Figure 13: Engine speed

It can also be observed that the power level obtained from the hybrid primary unit reaches the predicted values in the simulation study of section 4, which indicates that the engine

management algorithm effectively controls the engine speed, as shown in Figure 13, and the hybrid controller effectively controls the accumulator state-of-charge. Also important to note is the primary unit displacement. It can be observed that as power demand from the DC actuators increases above the maximum prescribed value, the displacement rapidly moves over-center to force the machine into motoring mode. When no more power assistance is required, the unit returns to charge the accumulator, which is reflected in the accumulator state-of-charge shown in **Figure 12**. Finally and most important, from **Figure 11**, it can be seen that the engine operation is wide-spread over the range of allowable speeds and torques having two main concentrations, one at speeds between 2550 and 2750 rpm, which is a result of satisfying the DC actuators performance, and another one at speeds between 1800 and 2200 rpm, which is a result of operating the machine at the most efficient point given the load when the operator commands allow it.

It must be noted that the developed control algorithm does not seek to achieve machine optimal operation. In order to achieve this, the operator commands must be known a priori or a learning or model-based algorithm must be implemented to focus on maintaining the mean accumulator pressure at the lowest possible while still maintaining operability. This then would allow the engine to operate at lower speeds and the primary and secondary units to operate at lower pressures thereby incurring in lower losses. Nonetheless, the derived algorithms demonstrate that the hydraulic hybrid architecture in combination with DC actuation allows engine downsizing by up to 55% for an excavator.

6. Conclusions

The presented results show the effectiveness of the developed control algorithms and demonstrate that the proposed algorithms results in the promised architecture engine downsizing. The derived controls are non-model based approaches which rely on measurements of the engine speed, the hybrid accumulator state-of-charge and the hydraulic units' displacements to distribute the power in the system according to its operation. The power management algorithms formulation is generalized for DC multi-actuator machines with secondary-controlled hydraulic hybrid architectures, which makes them implementable for similar mobile equipment with distinct architecture configurations and/or applications. Future work may include more advanced algorithms such as learning schemes that can exploit the architecture and result in the highest possible fuel savings.

7. References

/1/ "Komatsu introduces the world's first hydraulic excavator," 2008. [Online]. Available: http://www.komatsu.com/CompanyInfo/press/2008051315113604588.html.

/2/ H. Inoue, "Introduction of PC200-8 Hybrid Hydraulic Excavators," in Komatsu Technical Report, 2008.

/3/ M. Kagoshima, M. Komiyama, T. Nanjo und A. Tsutsui, "Development of new hybrid excavator," 2007. [Online]. Available: http://www.kobelco.co.jp/english/ktr/pdf/ktr_27/039-042.pdf.

/4/ "Caterpillar Unveils First Hybrid Excavator," CAT, 2012. [Online]. Available: http://www.cat.com/en_US/news/press-releases/caterpillar-unveilsfirsthybridexcavator.html.

/5/ J. Zimmermann, Toward Optimal Multi-Actuator Displacement Controlled Mobile Hydraulic Systems, West Lafayette: Purdue University, 2012.

/6/ H. Nikolaus, "Antriebssystem mit hydrostatischer Kraftübertragung." Germany Patent Pat. P 27 39 968.4, 1977.

/7/ K. Petterson and S. Tikkanen, "Secondary Control in Construction Machinery – Design and Evaluation of an Excavator Swing Drive," The 11th Scandinavian International Conference on Fluid Power, SICFP'09, June 2-4, 2009, Linköping, Sweden.

/8/ R. Hippalgaonkar, Power Management Strategies for Hydraulic Hybrid Multi-Actuator Mobile Machines with DC Actuators, West Lafayette: Purdue University, 2014.

/9/ J. Grabbel und M. Ivantysynova, An Investigation of Swash Plate Control Concepts for Displacement Controlled Actuators, International Journal of Fluid Power, Bd. 6, No. 2, pp. 19 - 36, 2005.

/10/ J. Heywood, Internal Combustion Engines Fundamentals, New York: McGraw-Hill Book Company, 1988.

/11/ C. Williamson, Power Management for Multi-Actuator Mobile Machines with Displacement Controlled Hydraulic Actuators, West Lafayette: Purdue University, 2010.

/12/ E. Busquets und M. Ivantysynova, A Gain-Scheduled Approach for the Engine Anti-Stall Control of Displacement-Controlled Multi-Actuator Systems, Elsevier Control Engineering Practice, (Under review).